Tribology Letters (2020) 68:96
https://doi.org/10.1007/s11249-020-01327-4

ORIGINAL PAPER

Influence of Interstitial Oxygen on the Tribology of Ti6Al4V

Daniel Kümmel[1,3] · Johannes Schneider[1,3] · Peter Gumbsch[1,2,3]

Received: 24 April 2020 / Accepted: 4 August 2020 / Published online: 5 September 2020

Abstract
Titanium alloys are used for their good mechanical and corrosion properties, but generally experience poor wear behavior. This can effectively be counteracted by a thermal oxidation treatment, reducing wear significantly. Employing a special sample preparation, we study the transition of tribological properties between thermally oxidized and bulk Ti6Al4V on a single sample. While oxygen signal intensity and hardness followed an exponential decay from the surface to bulk material, tribological results showed a step-like transition from low to high friction and wear with increasing distance from the surface. Low wear was associated with minor abrasive marks, whereas high wear showed as severe adhesive material transfer onto the steel counter body. Besides the mechanical property of hardness, also a change in fracture behavior by interstitial oxygen could influence the observed tribological behavior.

Keywords Adhesive wear · Aviation · Boundary lubrication · EDS · Surface modification · Titanium

1 Introduction

Titanium alloys are heavily used for their high specific strength and good corrosion resistance. Their high strength-to-weight ratio makes them desirable materials especially in aerospace industry [1]. Their excellent corrosion resistance yields good biocompatibility which, together with high strength, makes them appicable in biomedical industry [2]. The α/β-alloy Ti6Al4V is by far the most commonly used titanium alloy [3]. A major drawback of titanium alloys are the notoriously poor tribological properties like high, unsteady friction [4] and low wear resistance [5]. In most cases, distinct signs of adhesive wear are observed, like deep craters and material transfer to the counter body, which result in high wear rates [6, 7]. In many applications, the use of titanium alloys is therefore considered to be restricted to non-tribological parts [8]. In order to overcome this limitation, many different methods of surface engineering have been used on titanium alloys in order to improve their tribological properties. For instance, mechanical treatments like shot peening, burnishing, laser peening have been used in order to induce residual compressive stresses or nanocrystalline surface layers [9–12]. Furthermore, different types of hard coatings like Cr, CrN, NiP, TiN or DLC [5, 9, 13–15] or soft coatings like solid lubricants [5, 16] have been applied in order to reduce wear on titanium alloys.

Several methods of introducing interstitial atoms were successful in reducing wear on titanium alloys, such as ion implantation [17–19] or thermochemical treatments like nitriding and carburizing [20–22]. Also laser-induced chemical changes in Ti6Al4V can lead to significant improvements in its tribological behavior [23, 24]. It appears that adhesive wear can be avoided and wear volume reduced by more than two orders of magnitude. Similarly, thermal oxidation can produce an oxygen-rich diffusion layer at the surface and similar reductions in wear are reported [25, 26]. It should be noted that besides a nm-thin passivation layer, no thick titanium oxide layer was reported for these experiments. Observed differences in tribological behavior are therefore supposedly based on the changed material chemistry of metallic subsurface Ti6Al4V. Interstitial oxygen appears to be the key component.

Most of the mentioned surface treatments are only available categorically, e. g. “coated” or “non-coated”. In this paper, we explicitly investigate the *transition* in tribology depending on the concentration of interstitial oxygen

✉ Johannes Schneider
johannes.schneider@kit.edu

[1] Institute for Applied Materials IAM, Karlsruhe Institute of Technology KIT, Karlsruhe, Germany

[2] Fraunhofer Institute for Mechanics of Materials IWM, Freiburg, Germany

[3] MicroTribology Center μTC, Karlsruhe, Germany

in Ti6Al4V instead. We make use of the oxygen gradient underneath the surface produced by thermal oxidation. By grinding the surface of a sample under a small angle, different material composition and different properties can be observed at different locations. The influence of of this gradient on friction and wear behavior will be reported.

2 Experimental

2.1 Materials and Sample Preparation

Tribological testing was performed in a lubricated contact in linear reciprocating motion with 100Cr6 cylinders on a Ti6Al4V plate. The Ti6Al4V material was supplied in an annealed state by ARA-T (Dinslaken, Germany). It showed an equiaxed microstructure and a macroscopic hardness of 325 HV3 in bulk. A plate of the dimensions Ø25 mm x 8 mm was first ground with a diamond grinding wheel D91 on a cup grinding machine (G&N MPS 2 R300, Nürnberg, Germany) under continuous supply of coolant to ensure maximum surface evenness and parallelism. The sample was then further ground omnidirectionally on a Buehler PowerPro 4000 metallographic grinding machine (Esslingen, Germany) with a 240 grit SiC paper under constant water supply. For thermal oxidation, the sample was then placed in a Nabertherm muffle furnace (Lilienthal, Germany) for two hours at 800 °C and subsequently cooled outside the furnace in air. A series of dimples was created by laser ablation near the edge of the top surface. The depth of each of these dimples was measured by confocal microscopy (Sensofar Plμ Neox, Barcelona, Spain) and used later for calculation of the inclination angle of the final surface.

Preparation of the final inclined surface of the sample was done with the same diamond grinding wheel D91. A 30 µm precision foil was put under one side of the sample in order to lift this side for grinding (Fig. 1a). This led to the inclined surface. Grinding marks are oriented parallel to the surface gradient and therefore perpendicular to the prospective sliding direction. Roughness determined by confocal microscope was $R_a = 0.36$ µm. After grinding the inclined surface, laser dimples were again measured by confocal microscopy. Comparing each dimple depth before and after grinding, the inclination of the resulting surface of around 0.075° could be determined with a high accuracy of ± 0.005°. Additionally, the topography of the whole sample was measured by the optical profilometer FRT Microprof 100 (Bergisch Gladbach, Germany).

Cylinder rollers (SKF, Schweinfurt, Germany) of Ø10 mm x 10 mm made from 100Cr6 steel were used as counter bodies for the tribological experiments. Cylinder surface roughness R_a was around 0.15 µm. The microstructure consists of annealed martensite, resulting in an average hardness of 750 HV3.

All samples were cleaned in an ultrasonic bath using petroleum spirit and ethanol for 10 min each, directly before the experiments.

As lubricant for the tribological experiments, AeroShell Grease 33 (Shell, Hamburg, Germany) was used, which has a base oil viscosity of 14.2 mm^2/s and 3.4 mm^2/s at 40 °C and 100 °C, respectively. AeroShell Grease 33 is a universal aerospace grease which contains corrosion/oxidation inhibitors and load carrying additives in a lithium complex thickened synthetic base oil.

2.2 Characterization Methods

For nanoindentation measurements and microstructural characterization, an equally thermally oxidized sample was embedded in a polymeric resin mixed with conductive nickel filler. A metallographic cross section was prepared by grinding up to 4000 grit SiC paper and subsequent polishing with 6 µm, 3 µm and 1 µm diamond paste. Final chemical–mechanical polishing was done using a mixture of 90 ml OP-U suspension and 10 ml 30% H_2O_2.

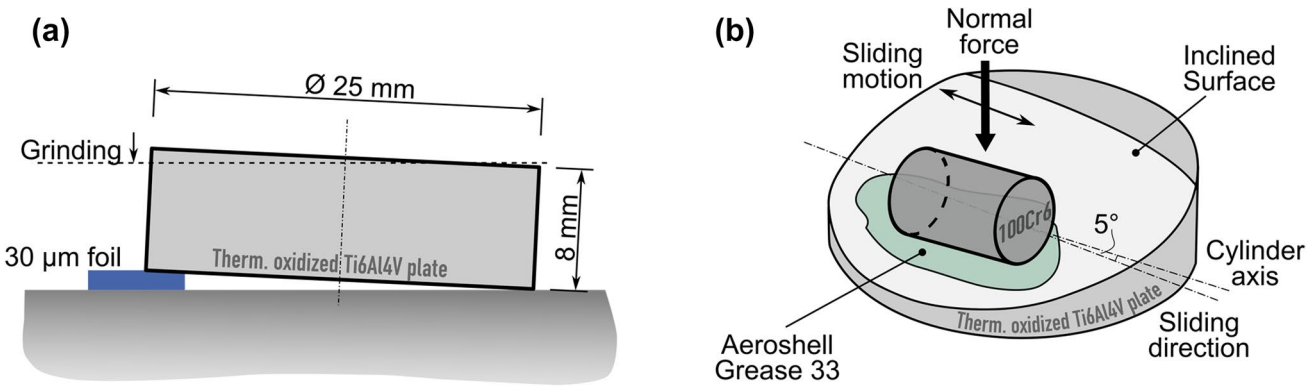

Fig. 1 Schematic representation of the manufacturing of the inclined surface (**a**) and the realization of tribological experiments (**b**)

Nanoindents were performed on a Hysitron TI 950 Triboindenter (Minneapolis, USA) with a modified Berkovich indenter tip and a load of 9 mN. Indenter area function was calibrated before the measurements by indents in fused silica.

For the microstructural characterization of the treated surface and observation of wear scars, the electron beam imaging of a FEI Helios Nanolab 650 Dual Beam Microscope (Hillsboro, USA) was used. Energy dispersive X-ray spectroscopy (EDX) maps were acquired at the same microscope with a X Max 80 silicon drift detector (Oxford Instruments, Abingdon, UK).

Depth-resolved chemical composition was characterized by glow discharge optical emission spectroscopy (GDOES) in a Leco GDS 850A spectrometer (St. Joseph, USA). Due to the lack of reference materials, these measurements only give qualitative information on the chemical composition. Sputter rate was determined after the measurement by measuring the crater depth with confocal microscopy.

Tribological experiments were conducted on an Optimol SRV reciprocating tribometer (Munich, Germany) as shown in Fig. 1b. The experimental parameters are summarized in Table 1. Sliding direction was perpendicular to the grinding marks and the surface gradient. Cylindrical counter bodies were oriented with their cylinder axis under 5° to the sliding direction and parallel to the surface. Grease was applied with a little spatula, without touching the surfaces with the spatula itself. Contacts were greased excessively, immediately before the experiment, to ensure lubrication of the whole contact throughout the entire experiment.

In wear scars with high and medium amounts of wear, wear volumes could be directly calculated from the confocal image. For experiments with low wear, wear depth was below the surface roughness and no wear volume could be calculated directly. However, a wear scar was visible in light microcopy (Keyence VHX 600D, Osaka, Japan) by a slight color change. The upper limit of wear volume was therefore estimated by the area of the wear scar multiplied by the arithmetic average height R_a.

Table 1 Parameters of the tribological experiments

Parameter	Unit	Value
Base body		Ti6Al4V plate with inclined surface
Counter body		100Cr6 steel cylinder rollers, Ø10 mm × 10 mm
Lubricant		Aeroshell Grease 33
Atmosphere		25 ± 3 °C and 50 ± 5% RH
Normal load	N	20
Frequency	Hz	20
Stroke	mm	0.2
Duration	min	60
Sliding distance	m	28.8

3 Results

Figure 2 shows the results of topographic characterization of the tribological sample before the experiment as well as chemical and mechanical characterization of the corresponding thermally oxidized material. The 3D topography image in Fig. 2a) shows the sample surface, which is inclined with respect to the sample but has a high evenness within itself. On the top right side, a part of the plate was left unground as a reference. Inclination angle was determined by three independent methods: comparison of laser dimple depths before and after grinding, large area topography scan (Fig. 2a) and by measuring the sample thickness with

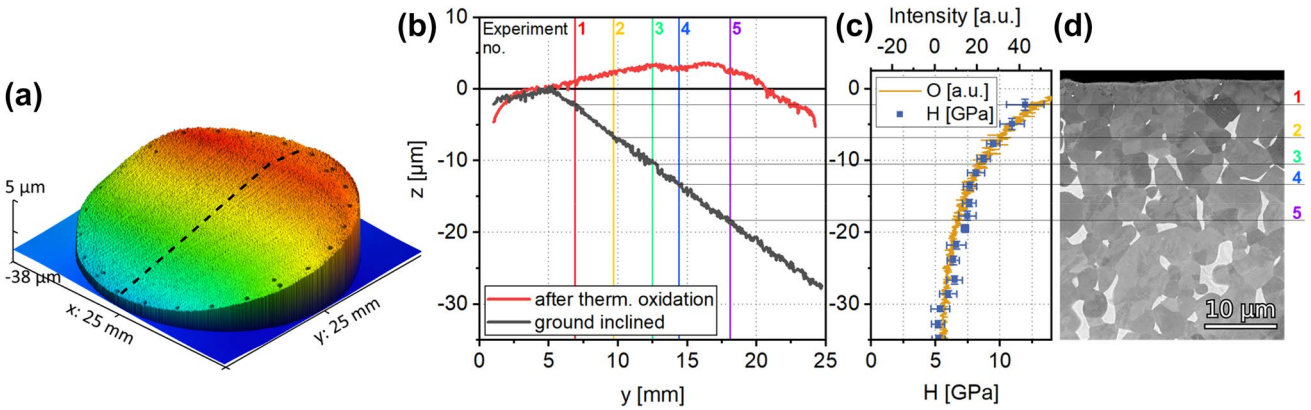

Fig. 2 Characterization of the prepared tribological sample: **a** 3D topography image of the inclined surface **b** topographic profile drawn along the line in (**a**), vertical and horizontal lines indicate the positions of tribological experiments. **c** Oxygen content (O) and hardness (H) versus the distance from the surface **d** cross-sectional microstructure of the corresponding thermally oxidized material

a micrometer screw. All methods agreed well and showed that the surface was inclined by around 0.075°. The surface profile along the dashed black line in Fig. 2a is given in Fig. 2b, together with the profile of the sample after oxidation but before grinding. Locations of the prospective tribological experiments are marked by vertical lines with the numbers 1–5. This color scheme of red to purple according to the position of the experiment on the sample is also used in the following results. Figure 2c shows depth resolved measurements of nanoindentation hardness and GDOES oxygen signal intensity. Both follow an exponential decay from the surface, the hardness with a peak value of 12 GPa near the surface compared to 5.2 GPa in bulk, which agrees well with previous studies [25, 27]. GDOES signal intensity can only be interpreted qualitatively, since intensity not only depends on atomic concentration but also other factors such as emission yield and sputter rate [28, 29]. However, several authors correlated the hardness of Ti6Al4V with an absolute concentration of oxygen [27, 30]. Using these correlations, we can estimate that the concentration of oxygen in the relevant depth should be in the order of several at%. An SEM image of the cross-sectional microstructure is shown in Fig. 2d. At the bottom of the image, bulk α/β-microstructure of Ti6Al4V can be observed. The fraction of β-phase (brighter grains) clearly decreases towards the surface, which is caused by the α-stabilizing characteristics of oxygen in titanium [3]. No oxides could be observed beneath the surface at any given magnification. This is in line with similar studies [25], including transmission electron microscopy investigations [31] and relates to the high maximum solubility of 33 at% oxygen in titanium [32].

Figure 3 illustrates the results of tribological experiments. Figure 3a shows the evolution of the friction coefficient of all five experiments conducted. Experiments 1 and 2 showed a constant coefficient of friction (CoF) of 0.12 throughout the whole experiment. Experiment 3 showed a slightly higher, but also constant CoF of 0.13. In contrast, experiments 4 and 5 revealed a distinct running-in behavior, with high and wildly fluctuating CoF over 0.5 in the beginning. Both exhibited a sudden transition to a constant CoF of 0.13 at a sliding distance of 10.7 m and 8.4 m, respectively. Figure 3b summarizes the tribological results as a function of the distance from the initial surface. For friction, the average CoF during the first 5 m of sliding distance was used as the initial CoF. For wear, both wear scar volume and wear scar area on Ti6Al4V are plotted. All three measures describe a similar trend: while experiments 1 and 2 exhibited low friction and negligible wear, experiments 4 and 5 exhibited higher initial friction and high wear. Variations in friction coefficient increase in the same fashion, as indicated by the error bars. Experiment 3 shows intermediate values of friction and wear, however clearly closer to the lower values of experiments 1 and 2. While the transitions of friction and wear may be perceived as similar and look alike in Fig. 3b, relative changes are different. For example, experiment 1 experienced 69.0% lower initial friction than experiment 5, however showed a 91.3% smaller wear area and 99.4% smaller wear volume.

In order to further characterize the wear behavior of experiments, wear scars were examined by scanning electron microscopy (SEM) and energy dispersive X-ray spectroscopy (EDX). Representative results are shown in Fig. 4, with the three columns signifying experiments 1, 3 and 5, respectively. Different rows show the tribological base body and counter body as captured by different detectors of the SEM. Wear scars on the base body were imaged by the secondary electron (SE) signal, in order to get a detailed depiction of the topography. The counter body was imaged by backscatter

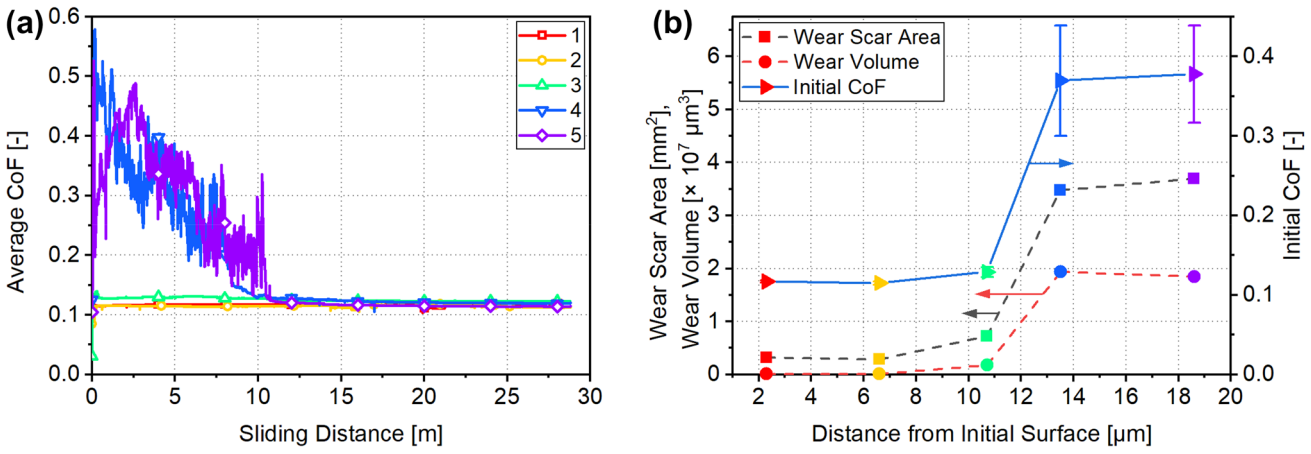

Fig. 3 Results of the tribological experiments: **a** Coefficient of friction over sliding distance for all five conducted experiments. **b** Initial coefficient of friction (averaged from the first 5 m of sliding distance), wear area and wear volume on Ti6Al4V as a function of the distance from the initial surface

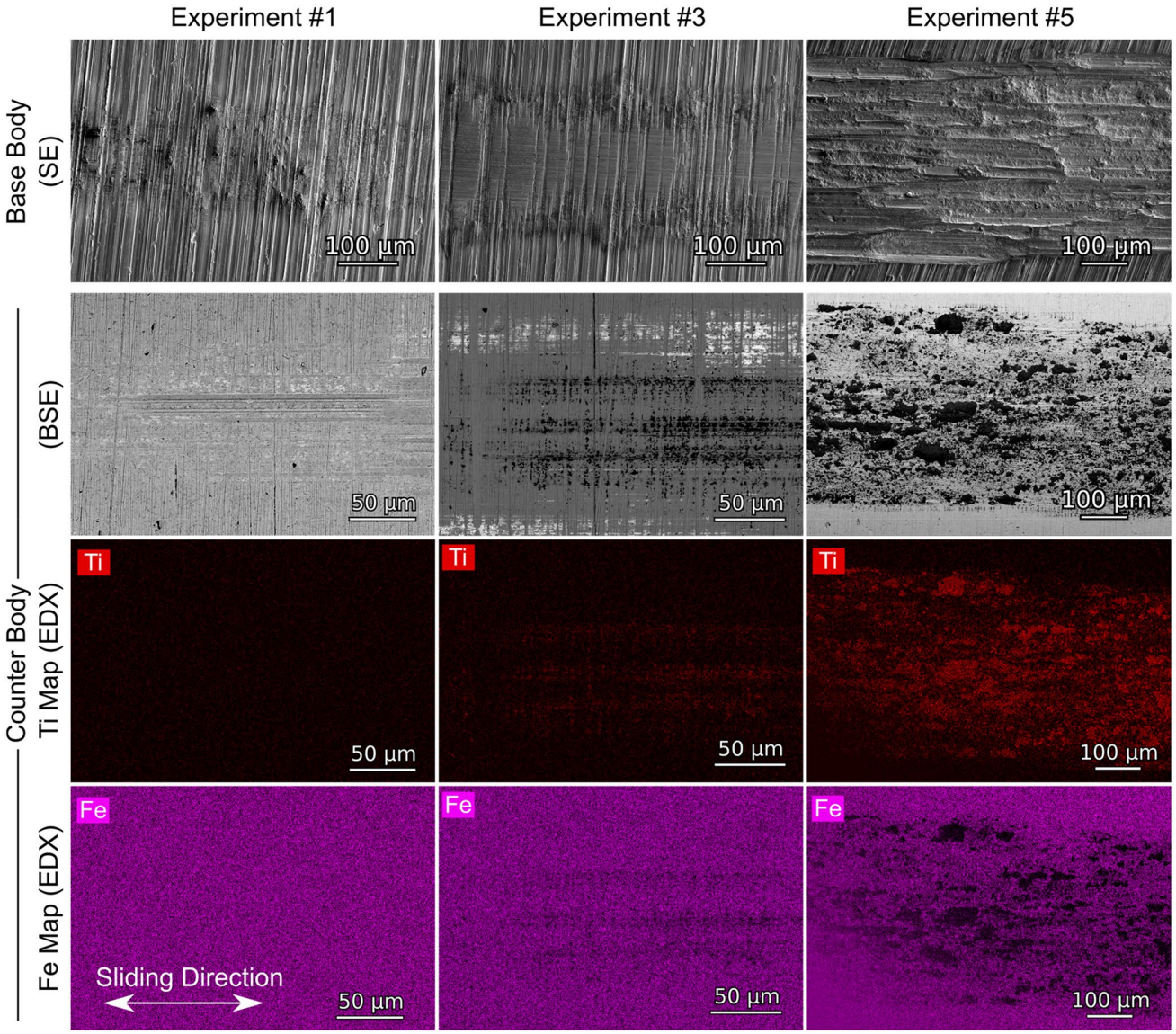

Fig. 4 Scanning electron microscopy study of worn surfaces: Columns correspond to experiments 1, 3 and 5 while each row shows different tribological body or detector. For some images, a different magnification was chosen in order to best capture the observed wear scar characteristics

electrons (BSE), so that possible material transfer from the base body could be seen more evidently. The same section of the counter body is shown in corresponding Ti- and Fe-EDX maps which are used to further clarify the origin of the transferred material. For some images, different magnifications were chosen in order to best capture the observed wear scar characteristics.

Wear scars of experiment 1 show minor signs of tribological loading. Only slight grooves and some particles can be observed. Also on the counter body, only slight abrasive marks are visible. Accordingly, the EDX maps show negligible Ti but high Fe contents, therefore no significant material transfer occurred. Base body wear scars of experiment 3 depict some clear plastic deformation, the topography which was left by grinding appears smoothed. Only by considering the counter body image, it becomes evident that small fragments (< 5 µm) of Ti6Al4V material were removed and transferred onto the steel counter body. This is further revealed by the EDX maps. However, the Ti transfer seems to be rather thin, since EDX-signal from the counter body underneath the transfer was still able to reach the detector. A completely different wear behavior is depicted by the base body wear scar of experiment 5. It shows distinct signs of severe adhesive wear like deep craters and grooves. The counter body shows fragments of different sizes (up to 100 µm) of Ti transfer. The thickness of these transferred fragments seems higher, since

no EDX-signal of the counter body reached the detector. These patches appear black in the Fe map, accordingly.

4 Discussion

A distinct interrelation of oxygen signal intensity, hardness, initial friction, wear volume and wear mechanisms became apparent in the tribological experiments on this specially prepared sample. Tribological loading of the oxygen-rich Ti6Al4V near the initial surface exhibited low friction and wear, whereas the on oxygen-lean Ti6Al4V showed high initial friction and high wear, as expected for a titanium alloy. The latter also showed greater variations in the CoF and wear was dominated by adhesion and material transfer. Experiment 3 revealed an interesting intermediate state, which clearly experienced adhesive wear, but not to the 'catastrophic' extend which is typical for titanium alloys [5, 25].

A separation into states of high and low wear has similarly been observed for surface treated titanium alloys before [9]. This can be related to the striking influence of the adhesive wear mechanism. If an adhesive junction between the two contacting bodies is formed, adhesive wear will lead to the removal and transfer of a part of the cohesively less strong body. In case of the experiments shown here, transfer occurred from Ti6Al4V onto 100Cr6. Thereby freshly exposed material is (initially) free from adhesion-inhibiting oxide- or boundary lubrication layers. Besides, for a graded surface (like that of thermal oxidation), the underlying material is 'less treated', thus less hard and chemically more reactive. Adhesive wear can therefore proceed more easily; a single adhesive junction in the beginning could potentially lead to severe adhesive wear over the course of the experiment.

The evolution of adhesive wear in general should be governed by three major factors of influence: the real contact area and the work of adhesion (which together determine an effective surface energy) and the resistance to the propagation of cracks. These influences are discussed in the following.

The real contact area is closely related to the near-surface mechanical properties of the two contacting bodies, specifically the yield strength. Hardness (and therefore yield strength) of the measured Ti6Al4V directly correlates with the oxygen intensity, which can be seen from Fig. 2c. Since no oxides were observed below the surface, this hardening is caused by solid solution strengthening, which is quite pronounced and well documented for oxygen in titanium [27, 33–37]. Hardness therefore follows closely the exponential decrease of oxygen intensity from the surface. The hardness of materials is also commonly accepted as a major influence on their wear resistance [38]. Especially for materials which are prone to adhesive wear (like titanium alloys), near-surface mechanical properties are deemed tribologically crucial since a higher hardness limits junction growth in tribological contact and therefore reduces the real contact area and adhesive forces [31, 39]. It was therefore somewhat unexpected that tribological results did not follow the exponential depth dependence of hardness, but showed a step-like transition (Fig. 3b) instead.

The work of adhesion also plays a role in the "stickiness" of the two contacting bodies. Speculatively, the chemical bonding characteristics and therefore the intrinsic work of adhesion between the two bodies could be affected by the presence of oxygen just like interface energies [23, 24, 40]. However, such electronic effects are usually small and certainly not abrupt.

Therefore, other factors than just hardness and the effective surface energy must influence the tribological response. This is also supported by experiments on nanocrystalline titanium which give much higher hardness but mixed tribological results and still show signs of adhesive wear [12, 41–44]. The correlation of increasing contact size and increasing adhesive forces with decreasing hardness certainly remains one effect.

Lastly, the formation of a wear particle by the adhesive wear mechanism requires the propagation of cracks and should therefore be closely related to materials fracture behavior. In the most simplistic picture of a sliding contact asperity, the contact can be regarded as two propagating mode II cracks in the front and the back of the contact and the sliding interface. Therefore, the decohesion of two contacting tribological bodies can be perceived as the propagation of a mode II crack [45]. The deviation of the crack path of either of the mode II cracks from the interface would then lead to adhesive wear. Comparing a tribological contact to a crack in a bi-material interface, the deflection of the crack can already be changed solely by tuning elastic constants of the two materials [46]. The stiffer oxygen-rich Ti6Al4V [35] would lead to less pronounced crack deflection compared to more compliant bulk Ti6Al4V. Adding plasticity to the concept, the development of the plastic zone in front of the crack tip becomes crucial. In a static scenario, the size of the plastic zone is determined by the yield strength of the material, which in titanium (alloys) strongly increases with increasing oxygen content [33–36, 47]. In a dynamic fracture scenario (due to continuous sliding) and on the microscopic level, dislocation mobility becomes the determining quantity [48]. Interstitial oxygen leads to reduced dislocation mobility [36, 49]. At a given strain rate, dislocations might no longer be able accommodate the plastic strain, which then leads to brittle fracture. Such decrease of fracture toughness with increasing oxygen concentration is also reported for titanium [50–53]. By analogy, the transition in tribological properties of Ti6Al4V can therefore be compared to a ductile to brittle transition where the change in dislocation mobility rather than just the yield strength determines the brittle to ductile transition [48]. In many other materials

such brittle to ductile transition is provoked e.g. by lowering temperature or increasing strain rate [48, 54]. Such analogy between fracture and tribology was previously also attempted by Buckley [55] and Bowden and Childs [56]. With the particularly abrupt change in adhesive wear for Ti6Al4V with oxygen content, such analogy to the brittle to ductile transition is particularly striking.

In short, the adhesive removal of a wear particle can be characterized by two competing processes of brittle crack propagation and plastic deformation. The transition critically depends upon dislocation mobility, which is markedly influenced by interstitial oxygen content. For the analysis of adhesive wear such change in fracture mode means that for brittle fracture at high oxygen the two contacting surfaces can cleanly decohere at the interface between the two bodies, while low oxygen allows more ductility and the crack path and failure mode can deviate from the interface and allow material transfer to the counter body. This clearly is compatible with all our observations. Further studies and quantitative modelling will be necessary to clarify the connection of fracture behavior and wear.

5 Conclusion

A Ti6Al4V sample was thermally oxidized and ground under a small angle in order to reveal different material properties at different locations of the sample. This was used to study the effects of interstitial oxygen on the tribological behavior of Ti6Al4V. A strong transition was observed concerning friction, amount of wear and wear scar morphology. While oxygen signal intensity and hardness followed an exponential decay from the surface, tribological results of the five experiments showed a step-like transition. Two experiments exhibited severe adhesive wear and high friction while two other exhibited negligible wear and low friction. The experiment in the middle marked the transition, with also low friction but measurable, small amounts of wear. Besides hardness, a mechanism based on the change in fracture behavior of oxygen-rich titanium may explain the tribological behavior.

Acknowledgements This work was funded by the German BMWi within the scope of the project FAWIBO (20Y1505C), headed by Liebherr-Aerospace. The authors thank Monika Rinke (KIT, IAM) for support with the GDOES measurements and Dominic Linsler (Fraunhofer IWM) for nanoindentation measurements.

Funding Open Access funding provided by Projekt DEAL.

References

1. Boyer, R.R.: An overview on the use of titanium in the aerospace industry. Mater. Sci. Eng.: A (1996). https://doi.org/10.1016/0921-5093(96)10233-1
2. Long, M., Rack, H.J.: Titanium alloys in total joint replacement—a materials science perspective. Biomaterials (1998). https://doi.org/10.1016/S0142-9612(97)00146-4
3. Lütjering, G., Williams, J.C.: Titanium 2 Engineering materials and processes. Springer, Berlin, Heidelberg (2007)
4. Dong, H.: Tribological properties of titanium-based alloys. In: Dong, H. (ed.) Surface engineering of light alloys. Aluminum, magnesium and titanium alloys. Woodhead Publishing in materials, pp. 58–80. Woodhead Publishing Limited, Oxford, UK (2010)
5. Budinski, K.G.: Tribological properties of titanium alloys. Wear (1991). https://doi.org/10.1016/0043-1648(91)90249-T
6. Fellah, M., Labaïz, M., Assala, O., Dekhil, L., Taleb, A., Rezag, H., Iost, A.: Tribological behavior of Ti-6Al-4V and Ti-6Al-7Nb alloys for total hip prosthesis. Adv. Tribol. (2014). https://doi.org/10.1155/2014/451387
7. Qu, J., Blau, P.J., Watkins, T.R., Cavin, O.B., Kulkarni, N.S.: Friction and wear of titanium alloys sliding against metal, polymer, and ceramic counterfaces. Wear (2005). https://doi.org/10.1016/j.wear.2004.09.062
8. Dong, H., Bell, T.: Enhanced wear resistance of titanium surfaces by a new thermal oxidation treatment. Wear (2000). https://doi.org/10.1016/S0043-1648(99)00359-2
9. Bansal, D.G., Eryilmaz, O.L., Blau, P.J.: Surface engineering to improve the durability and lubricity of Ti–6Al–4V alloy. Wear (2011). https://doi.org/10.1016/j.wear.2010.11.021
10. Golden, P.J., Hutson, A., Sundaram, V., Arps, J.H.: Effect of surface treatments on fretting fatigue of Ti–6Al–4V. Int. J. Fatigue (2007). https://doi.org/10.1016/j.ijfatigue.2006.10.005
11. Fu, Y., Loh, N.L., Batchelor, A.W., Liu, D., Zhu, X., He, J., Xu, K.: Improvement in fretting wear and fatigue resistance of Ti–6Al–4V by application of several surface treatments and coatings. Surf. Coat. Technol. (1998). https://doi.org/10.1016/S0257-8972(98)00528-3
12. Garbacz, H. (ed.): Nanocrystalline titanium micro & nano technologies series. Elsevier, San Diego (2019)
13. Podgornik, B., Hogmark, S., Sandberg, O.: Proper coating selection for improved galling performance of forming tool steel. Wear (2006). https://doi.org/10.1016/j.wear.2005.09.005
14. Wiklund, U., Hutchings, I.M.: Investigation of surface treatments for galling protection of titanium alloys. Wear (2001). https://doi.org/10.1016/S0043-1648(01)00730-X
15. Łępicka, M., Grądzka-Dahlke, M.: Surface modification of Ti6Al4V titanium alloy for biomedical applications and its effect on tribological performance-a review. Rev. Adv. Mater. Sci. **46**, 86–103 (2016)
16. Ripoll, M.R., Simič, R., Brenner, J., Podgornik, B.: Friction and lifetime of laser surface-textured and MoS2-coated Ti6Al4V under dry reciprocating sliding. Tribol. Lett. (2013). https://doi.org/10.1007/s11249-013-0170-6
17. Oñate, J.I., Alonso, F., García, A.: Improvement of tribological properties by ion implantation. Thin Solid Films (1998). https://doi.org/10.1016/S0040-6090(97)00564-6

18. Buchanan, R.A., Rigney, E.D., Williams, J.M.: Ion implantation of surgical Ti-6Al-4V for improved resistance to wear-accelerated corrosion. J. Biomed. Mater. Res. (1987). https://doi.org/10.1002/jbm.820210308
19. Oliver, W.C., Hutchings, R., Pethica, J.B.: The wear behavior of nitrogen-implanted metals. Metall. Trans. A (1984). https://doi.org/10.1007/BF02647105
20. Zhecheva, A., Sha, W., Malinov, S., Long, A.: Enhancing the microstructure and properties of titanium alloys through nitriding and other surface engineering methods. Surf. Coat. Technol. (2005). https://doi.org/10.1016/j.surfcoat.2004.07.115
21. Izman, S., Abdul-Kadir, M.R., Anwar, M., Nazim, E.M., Rosliza, R., Shah, A., Hassan, M.A.: Surface modification techniques for biomedical grade of titanium alloys: oxidation, carburization and ion implantation processes. In: Amin, A.K.M.N. (ed.) Titanium alloys—towards achieving enhanced properties for diversified applications. IntechOpen, London (2012)
22. Cheng, K.Y., Pagan, N., Bijukumar, D., Mathew, M.T., McNallan, M.: Carburized titanium as a solid lubricant on hip implants. Corrosion, tribocorrosion and biocompatibility aspects. Thin Solid Films (2018). https://doi.org/10.1016/j.tsf.2018.08.048
23. Kümmel, D., Linsler, D., Schneider, R., Schneider, J.: Surface engineering of a titanium alloy for tribological applications by nanosecond-pulsed laser. Tribol. Int. (2020). https://doi.org/10.1016/j.triboint.2020.106376
24. Kümmel, D., Hamann-Schroer, M., Hetzner, H., Schneider, J.: Tribological behavior of nanosecond-laser surface textured Ti6Al4V. Wear (2019). https://doi.org/10.1016/j.wear.2019.01.079
25. Qu, J., Blau, P.J., Howe, J.Y., Meyer III, H.M.: Oxygen diffusion enables anti-wear boundary film formation on titanium surfaces in zinc-dialkyl-dithiophosphate (ZDDP)-containing lubricants. Scr. Mater. (2009). https://doi.org/10.1016/j.scriptamat.2009.02.009
26. Yazdi, R., Ghasemi, H.M., Abedini, M., Wang, C., Neville, A.: Oxygen diffusion layer on Ti–6Al–4V alloy: scratch and dry wear resistance. Tribol. Lett. (2019). https://doi.org/10.1007/s11249-019-1214-3
27. Zabler, S.: Interstitial Oxygen diffusion hardening—a practical route for the surface protection of titanium. Mater. Charact. (2011). https://doi.org/10.1016/j.matchar.2011.10.012
28. Bengtson, A., Nelis, T.: The concept of constant emission yield in GDOES. Anal. Bioanal. Chem. (2006). https://doi.org/10.1007/s00216-006-0412-7
29. Payling, R., Jones, D.G., Gower, S.A.: Quantitative analysis with d.c.- and r.f.-glow discharge spectrometry. Surf. Interface Anal. (1993). https://doi.org/10.1002/sia.740201206
30. Yazdi, R., Ghasemi, H.M., Wang, C., Neville, A.: Bio-corrosion behaviour of oxygen diffusion layer on Ti-6Al-4V during tribo-corrosion. Corros. Sci. (2017). https://doi.org/10.1016/j.corsci.2017.08.031
31. Dong, H., Li, X.Y.: Oxygen boost diffusion for the deep-case hardening of titanium alloys. Mater. Sci. Eng.: A (2000). https://doi.org/10.1016/S0921-5093(99)00697-8
32. Okamoto, H.: O–Ti (oxygen–titanium). J. Phase Equilib. Diffus. (2011). https://doi.org/10.1007/s11669-011-9935-5
33. Finlay, W.L., Snyder, J.A.: Effects of three interstitial solutes (nitrogen, oxygen, and carbon) on the mechanical properties of high-purity. Alpha Titan. JOM (1950). https://doi.org/10.1007/BF03399001
34. Jaffee, R.I., Ogden, H.R., Maykuth, D.J.: Alloys of titanium with carbon, oxygen, and nitrogen. JOM **2**, 1261–1266 (1950)
35. Conrad, H.: Effect of interstitial solutes on the strength and ductility of titanium. Prog. Mater. Sci. (1981). https://doi.org/10.1016/0079-6425(81)90001-3
36. Yu, Q., Qi, L., Tsuru, T., Traylor, R., Rugg, D., Morris, J.W., Asta, M., Chrzan, D.C., Minor, A.M.: Origin of dramatic oxygen solute strengthening effect in titanium. Science (2015). https://doi.org/10.1126/science.1260485
37. Vaché, N., Monceau, D.: Oxygen diffusion modeling in titanium alloys: new elements on the analysis of microhardness profiles. Oxid. Met. (2020). https://doi.org/10.1007/s11085-020-09956-9
38. Leyland, A., Matthews, A.: On the significance of the H/E ratio in wear control. A nanocomposite coating approach to optimised tribological behaviour. Wear (2000). https://doi.org/10.1016/S0043-1648(00)00488-9
39. Molinari, A., Straffelini, G., Tesi, B., Bacci, T.: Dry sliding wear mechanisms of the Ti6Al4V alloy. Wear (1997). https://doi.org/10.1016/S0043-1648(96)07454-6
40. Ghazisaeidi, M., Trinkle, D.R.: Interaction of oxygen interstitials with lattice faults in Ti. Acta Mater. (2014). https://doi.org/10.1016/j.actamat.2014.05.025
41. Alikhani Chamgordani, S., Miresmaeili, R., Aliofkhazraei, M.: Improvement in tribological behavior of commercial pure titanium (CP-Ti) by surface mechanical attrition treatment (SMAT). Tribol. Int. (2018). https://doi.org/10.1016/j.triboint.2017.11.044
42. Salehikahrizsangi, P., Karimzadeh, F., Enayati, M.H., Abbasi, M.H.: Investigation of the effects of grain size and nano-sized reinforcements on tribological properties of Ti6Al4V alloy. Wear (2013). https://doi.org/10.1016/j.wear.2013.05.008
43. Garbacz, H., Grądzka-Dahlke, M., Kurzydłowski, K.J.: The tribological properties of nano-titanium obtained by hydrostatic extrusion. Wear (2007). https://doi.org/10.1016/j.wear.2006.11.047
44. Amanov, A., Cho, I.-S., Kim, D.-E., Pyun, Y.-S.: Fretting wear and friction reduction of CP titanium and Ti–6Al–4V alloy by ultrasonic nanocrystalline surface modification. Surf. Coat. Technol. (2012). https://doi.org/10.1016/j.surfcoat.2012.06.046
45. Greiner, C., Schäfer, M., Popp, U., Gumbsch, P.: Contact splitting and the effect of dimple depth on static friction of textured surfaces. ACS Appl. Mater. Interfaces (2014). https://doi.org/10.1021/am500879m
46. Ming-Yuan, H., Hutchinson, J.W.: Crack deflection at an interface between dissimilar elastic materials. Int. J. Solids Struct. (1989). https://doi.org/10.1016/0020-7683(89)90021-8
47. Oh, J.-M., Lee, B.-G., Cho, S.-W., Lee, S.-W., Choi, G.-S., Lim, J.-W.: Oxygen effects on the mechanical properties and lattice strain of Ti and Ti-6Al-4V. Met. Mater. Int. (2011). https://doi.org/10.1007/s12540-011-1006-2
48. Hartmaier, A., Gumbsch, P.: Scaling relations for crack-tip plasticity. Philos. Mag. A (2002). https://doi.org/10.1080/01418610210000018160
49. Barkia, B., Couzinié, J.P., Lartigue-Korinek, S., Guillot, I., Doquet, V.: In situ TEM observations of dislocation dynamics in α titanium: effect of the oxygen content. Mater. Sci. Eng., A (2017). https://doi.org/10.1016/j.msea.2017.07.040
50. Nagai, K., Yuri, T., Ogata, T., Umezawa, O., Ishikawa, K., Nishimura, T., Mizoguchi, T., Ito, Y.: Cryogenic mechanical properties of Ti-6Al-4V alloys with three levels of oxygen content. ISIJ Int. (1991). https://doi.org/10.2355/isijinternational.31.882
51. Wasz, M.L., Brotzen, F.R., McLellan, R.B., Griffin, A.J.: Effect of oxygen and hydrogen on mechanical properties of commercial purity titanium. Int. Mater. Rev. (1996). https://doi.org/10.1179/imr.1996.41.1.1
52. Yoder, G.R., Cooley, L.A., Crooker, T.W.: Fatigue crack propagation resistance of beta-annealed Ti-6AI-4V alloys of differing interstitial oxygen contents. Metall. Mater. Trans. (1978). https://doi.org/10.1007/BF02661812
53. Bache, M.R., Evans, W.J., McElhone, M.: The effects of environment and internal oxygen on fatigue crack propagation Ti-6Al-4V. Mater. Sci. Eng., A (1997). https://doi.org/10.1016/S0921-5093(97)00402-4
54. Gumbsch, P., Riedle, J., Hartmaier, A., Fischmeister, H.F.: Controlling factors for the brittle-to-ductile transition in tungsten

single crystals. Science (1998). https://doi.org/10.1126/science.282.5392.1293
55. Buckley, D.H.: Effect of 3 1/2 percent silicon on adhesion, friction and wear of iron in various media. NASA TN D-5667 (1970)
56. Bowden, F.P., Childs, T.H.C.: The friction and deformation of clean metals at very low temperatures. Proc. R. Soc. Lond. A (1969). https://doi.org/10.1098/rspa.1969.0170